

## Analyzing power for proton elastic scattering from the neutron-rich ${}^6\text{He}$ nucleus

T. Uesaka,<sup>1,\*</sup> S. Sakaguchi,<sup>1</sup> Y. Iseri,<sup>2</sup> K. Amos,<sup>3</sup> N. Aoi,<sup>4</sup> Y. Hashimoto,<sup>5</sup> E. Hiyama,<sup>4</sup> M. Ichikawa,<sup>6</sup> Y. Ichikawa,<sup>7</sup> S. Ishikawa,<sup>8</sup> K. Itoh,<sup>9</sup> M. Itoh,<sup>6</sup> H. Iwasaki,<sup>7</sup> S. Karataglidis,<sup>10</sup> T. Kawabata,<sup>1</sup> T. Kawahara,<sup>11</sup> H. Kuboki,<sup>7</sup> Y. Maeda,<sup>12</sup> R. Matsuo,<sup>6</sup> T. Nakao,<sup>7</sup> H. Okamura,<sup>13</sup> H. Sakai,<sup>7</sup> Y. Sasamoto,<sup>1</sup> M. Sasano,<sup>7</sup> Y. Satou,<sup>5</sup> K. Sekiguchi,<sup>4</sup> M. Shinohara,<sup>5</sup> K. Suda,<sup>13</sup> D. Suzuki,<sup>7</sup> Y. Takahashi,<sup>7</sup> M. Tanifuji,<sup>8</sup> A. Tamii,<sup>13</sup> T. Wakui,<sup>6</sup> K. Yako,<sup>7</sup> Y. Yamamoto,<sup>14</sup> and M. Yamaguchi<sup>4</sup>

<sup>1</sup>Center for Nuclear Study, University of Tokyo, Tokyo 113-0033, Japan

<sup>2</sup>Department of Physics, Chiba-Keizai College, Chiba 263-0021, Japan

<sup>3</sup>School of Physics, University of Melbourne, Melbourne, Australia

<sup>4</sup>RIKEN Nishina Center, Saitama 351-0198, Japan

<sup>5</sup>Department of Physics, Tokyo Institute of Technology, Tokyo 152-8551, Japan

<sup>6</sup>Cyclotron & Radioisotope Center, Tohoku University, Miyagi 980-8578, Japan

<sup>7</sup>Department of Physics, University of Tokyo, Tokyo 113-0033, Japan

<sup>8</sup>Science Research Center, Hosei University, Tokyo 102-8160, Japan

<sup>9</sup>Department of Physics, Saitama University, Saitama 338-8570, Japan

<sup>10</sup>Department of Physics and Electronics, Rhodes University, Post Office Box 94 Grahamstown 6140, South Africa

<sup>11</sup>Department of Physics, Toho University, Chiba 274-8510, Japan

<sup>12</sup>Faculty of Engineering, University of Miyazaki, Miyazaki 889-2192, Japan

<sup>13</sup>Research Center for Nuclear Physics, Osaka University, Osaka 567-0047, Japan

<sup>14</sup>Tsuru University, Yamanashi 402-8555, Japan

(Received 27 May 2010; published 26 August 2010)

Vector analyzing power for the proton- ${}^6\text{He}$  elastic scattering at 71 MeV/nucleon has been measured for the first time, with a newly developed polarized proton solid target, which works at a low magnetic field of 0.09 T. The results are found to be incompatible with a  $t$ -matrix folding model prediction. Comparisons of the data with  $g$ -matrix folding analyses clearly show that the vector analyzing power is sensitive to the nuclear structure model used in the reaction analysis. The  $\alpha$ -core distribution in  ${}^6\text{He}$  is suggested to be a possible key for understanding the nuclear structure sensitivity.

DOI: [10.1103/PhysRevC.82.021602](https://doi.org/10.1103/PhysRevC.82.021602)

PACS number(s): 24.70.+s, 25.60.-t, 29.25.Pj

Spin observables in scattering experiments have been rich sources for our understanding of nuclear structure, reaction, and interactions. A good example is spin asymmetry in proton-proton and proton-nucleus ( $p$ - $A$ ) scatterings, which is a direct manifestation of spin-orbit coupling in the system. The first spin-asymmetry measurements carried out by use of a double scattering method [1,2] clearly demonstrated that the spin-orbit coupling in nuclei is an order of magnitude stronger than that caused by the relativistic effect [3]. At present, the spin-orbit coupling in  $p$ - $A$  scattering is quantitatively established through numerous experiments by using polarized proton beams for stable targets.

It is interesting to use spin-asymmetry measurements to study unstable nuclei. Nuclei that locate near the neutron drip line occasionally show distinctive structure such as halos or skins. The neutron-rich  ${}^6\text{He}$  nucleus is one of the typical nuclides with an extended neutron distribution. Since the extended neutron distribution is prominent at the nuclear surface and the spin-orbit coupling is, in nature, a surface phenomenon, it is stimulating to see how the extended neutron distributions affect the spin asymmetry (i.e., vector analyzing power) in proton elastic scattering.

In this Rapid Communication, we report new results of vector analyzing power for the  $p$ - ${}^6\text{He}$  elastic scattering at

71 MeV/nucleon, measured with a newly developed polarized proton target. The results are compared with microscopic folding model calculations.

Although cross sections in proton elastic scattering from  ${}^6\text{He}$  have been extensively measured over a wide range of energies [4–9], there have been no measurement of vector analyzing power until recently. Since unstable nuclei are produced as secondary beams, we need a polarized proton target, practically in the solid state, for the spin-asymmetry studies. In addition, the solid polarized proton target should work under a low magnetic field of  $B \sim 0.1$  T for detection of recoiled protons with magnetic rigidity as low as 0.3 Tm. The traditional dynamical nuclear polarization technique [10], which demands a magnetic field higher than a few Tesla, cannot be applied therefore. Although this difficulty might be overcome by applying a spin frozen operation, efforts to do so have not been successful so far. An alternative approach to overcome the problem is to develop a polarized target based on a new principle, which is independent of magnetic-field strength.

We have succeeded in constructing a new solid polarized proton target, which works at a low magnetic field of about 0.1 T [11]. Here, protons in the target are polarized by transferring electron polarization in photoexcited triplet states of pentacene molecules via cross polarization [12]. The magnitude of the electron polarization is 73% and depends neither on the magnetic-field strength nor on the temperature

\*uesaka@cns.s.u-tokyo.ac.jp

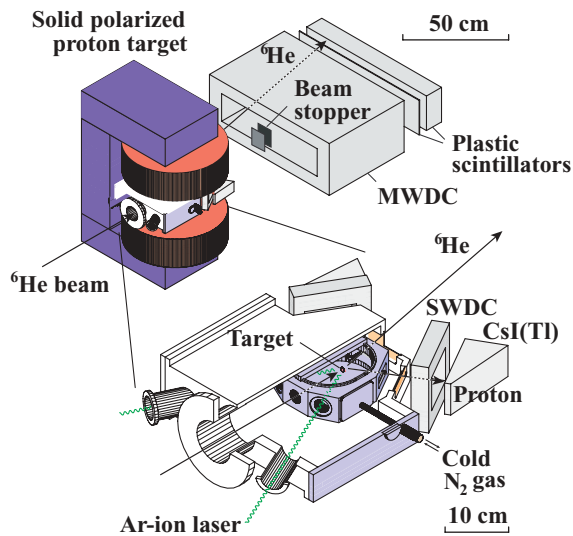


FIG. 1. (Color online) Schematic of the experimental setup, which includes the polarized proton solid target.

of the material. This makes it possible to operate the polarized target under a low magnetic field of 0.1 T and a high temperature of 100 K.

The first experiment with this target system was carried out in 2003 in which spin asymmetry in the  $p$ - ${}^6\text{He}$  elastic scattering was measured [13]. The data presented interesting features that were completely incompatible with theoretical predictions. From phenomenological optical model analyses, it was implied that the  $p$ - ${}^6\text{He}$  spin-orbit potential might extend to a larger radius compared with the  $p$ - ${}^6\text{Li}$  case. In Ref. [14], Crespo and Moro claim that an extended neutron distribution cannot be responsible for the large spin-orbit radius. Thus, connection between the spin-orbit potential in the  $p$ - ${}^6\text{He}$  scattering and the extended neutron distribution in  ${}^6\text{He}$  is still unclear. However, accuracy of the previous data is insufficient for further detailed and quantitative analysis. This is mainly because the analyzing power data were obtained with an assumed value of target polarization [13].

To obtain accurate analyzing power data with a reliable normalization, we have performed the  $p$ - ${}^6\text{He}$  spin-asymmetry experiment with upgraded target and detector systems.

The experiment was performed at RIKEN Accelerator Research Facility. The setup, which included the polarized target system, shown in Fig. 1, was placed downstream of the final focal plane of the RIKEN projectile fragment separator (RIPS) [15]. A radioactive  ${}^6\text{He}$  beam with an energy of  $70.6 \pm 1.4$  MeV/nucleon was produced via the projectile fragmentation reaction of a primary  ${}^{12}\text{C}$  beam on a  $1.39$  g/cm $^2$  beryllium target. An energy and an average intensity of the primary beam were 92 MeV/nucleon and 600 pnA, respectively. The resulting intensity and purity of the  ${}^6\text{He}$  beam was  $3.0 \times 10^5$  cps and 95%, respectively.

After separation in RIPS, the  ${}^6\text{He}$  beam bombarded the polarized target made of a crystal of naphthalene with a small amount ( $\sim 0.005$  mol %) of pentacene as a dopant. The dimensions of the target were 1 mm in thickness and 14 mm in diameter. The target was placed in a homogeneous magnetic

field of 0.09 T produced by a C-type magnet. The target chamber, which was thermally isolated from the room-temperature environment, was cooled down to 100 K by blowing cold nitrogen gas into it. Laser light from Ar-ion lasers irradiated the target to polarize electrons in pentacene molecules [16].

The relative magnitude of the proton polarization was monitored with a pulse NMR method during the measurement. The absolute value of the polarization was calibrated by comparing the NMR signal amplitude to the asymmetry of the  $p$ - ${}^4\text{He}$  scattering, measured with the same setup at 80 MeV/nucleon. The analyzing power data for the  $p$ - ${}^4\text{He}$  scattering in Ref. [17] were used in the calibration. The proton polarization was found to be  $20 \pm 4\%$  at maximum and  $14 \pm 3\%$  on average (see Ref. [11]). Statistical uncertainty in the  $p$ - ${}^4\text{He}$  measurement dominates the uncertainties in the proton polarization.

Scattered  ${}^6\text{He}$  particles were detected by a multiwire drift chamber (MWDC) and plastic scintillators placed about 1-m downstream of the target. Pulse-height information from the plastic scintillators is used to identify the particle. The  ${}^6\text{He}$  trajectory determined by the MWDC provides the scattering angle of the  ${}^6\text{He}$  and the reaction position on the target. Two counter telescopes to detect recoiled protons were placed left and right with respect to the beam axis. Each telescope was composed of a single-wire drift chamber for a position measurement and a CsI(Tl) scintillator for a total-energy measurement. They covered an angular range of  $\theta_{\text{c.m.}} = 35^\circ$ – $90^\circ$  in the center-of-mass system. The background around the elastic-scattering peak was reasonably small, which enables us to obtain yields of interest reliably.

The angular distributions of differential cross section ( $d\sigma/d\Omega$ ) and vector analyzing power ( $A_y$ ) are shown by filled circles in Fig. 2. Only statistical uncertainties are shown in the figure. Systematic uncertainty in  $A_y$ , mainly caused by uncertainty in absolute normalization of proton polarization, is 19% independent of scattering angles. The cross-section data are obtained with systematic uncertainty of 9% up to backward angles of  $\theta_{\text{c.m.}} \leq 87^\circ$ .

In the top panel of the figure, the data for the  $p$ - ${}^6\text{Li}$  elastic scattering [18] (triangles) are shown for comparison. As indicated in Ref. [13],  $d\sigma/d\Omega$  in the  $p$ - ${}^6\text{He}$  scattering is almost identical to that in the  $p$ - ${}^6\text{Li}$  scattering at  $\theta_{\text{c.m.}} \leq 50^\circ$ . This indicates that matter distributions in  ${}^6\text{He}$  and  ${}^6\text{Li}$  are similar, which is consistent with the recent results from GSI [8]. On the other hand, one can find small but apparent differences at backward angles  $\theta_{\text{c.m.}} > 50^\circ$ , which can be a manifestation of a halo structure in  ${}^6\text{He}$  [19].

In the lower panel of Fig. 2, we show the analyzing power for the  $p$ - ${}^6\text{He}$  elastic scattering at 71 MeV/nucleon, together with the  ${}^6\text{Li}$  data. In sharp contrast to the cross section, the  $A_y$  data for the  $p$ - ${}^6\text{He}$  scattering are quite different from that for  $p$ - ${}^6\text{Li}$ , especially at  $\theta_{\text{c.m.}} > 50^\circ$ . Dotted lines in Fig. 2 represent the prediction of the full  $t$ -folding optical potential model by Weppner *et al.* [20] reported before our measurement. This model calculates the  $p$ - $A$  scattering amplitudes by folding free nucleon-nucleon scattering amplitudes ( $t$ -matrix) based on the Nijmegen I interaction with off-shell density matrices. The calculations predict large positive values of analyzing power in the region of measurement independent of the nuclear structure

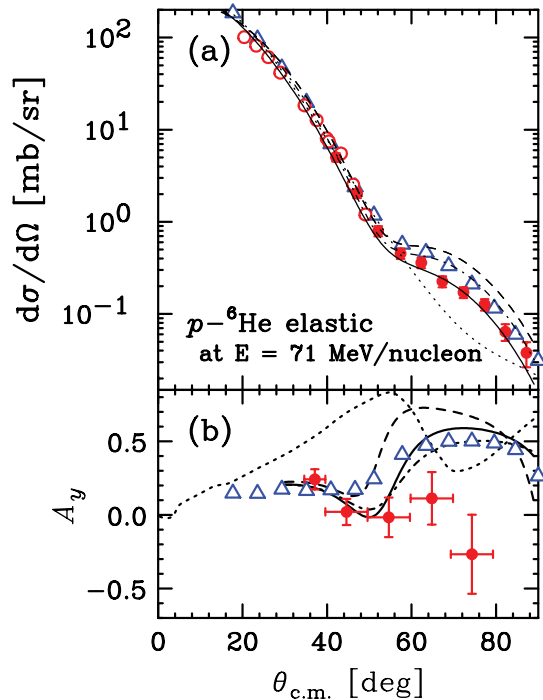


FIG. 2. (Color online) Cross section and vector analyzing power for the  $p$ - ${}^6\text{He}$  elastic scattering at 71 MeV/nucleon (filled circles), together with cross-section data in Ref. [4] (open circles) and data for  ${}^6\text{Li}$  [18] (triangles) targets. The dotted lines are a  $t$ -folding calculation in Ref. [20]. Results of 6BF calculations with harmonic oscillator (dashed), WS with (solid), and without halo (dot-dashed) single-particle wave functions are shown.

model used. The predicted angular distribution is clearly inconsistent with the present  $A_y$  data, while the calculation reasonably reproduces the cross-section data at forward angles. Those comparisons indicate that vector analyzing power can provide new information on the reaction mechanism and also on the nuclear structure, additional to that from the smaller scale effects in the elastic-scattering cross section.

To obtain a deeper understanding, we have compared the data with two different  $g$ -matrix folding model calculations: One is a full six-body folding (6BF) calculation [19,21], and the other is a cluster-folding (CF) calculation, which considers  ${}^6\text{He}$  to have an explicit  $\alpha$  core.

The  $g$ -matrix folding model, defined and used in Refs. [19,21], has been successful in describing  $p$ - $A$  elastic and inelastic scatterings for a wide range of nuclear masses and energies. In the model, the nonlocality of the  $p$ - $A$  interaction caused by an exchange term is taken into account in a fully microscopic way. Nuclear structure effects to the scattering are taken into account through single-particle wave functions, one-body density-matrix elements, and the  $g$ -matrix interaction. The  $g$ -matrix is obtained by solving the Bethe-Bruckner-Goldstone equations for the Bonn-B potential. Use of the  $g$ -matrix is the largest difference from that in Ref. [20]. Three curves in Fig. 2 represent results for different nuclear structure models: Solid and dot-dashed curves are results with a single-particle wave function for a Woods-Saxon (WS) potential with and without a halo component, respectively,

while dashed curves are for a harmonic oscillator potential. It is found that the predicted  $A_y$  varies by as much as 0.2, depending on the nuclear structure model used in the analysis. Overall agreement to the  $d\sigma/d\Omega$  and  $A_y$  data can be obtained with WS wave functions. In particular,  $d\sigma/d\Omega$  at  $\theta_{c.m.} > 50^\circ$  prefers a model with halo structure.

What is the origin of this sensitivity to nuclear structure? Is it caused by the *direct* valence neutron contribution or to the  $\alpha$ -core contribution, or both? Comparison with CF calculations is suited for clarifying the origin. Since the  ${}^6\text{He}$  nucleus is known to have a well-developed  $\alpha$ - $n$ - $n$  structure, a folded interaction of  $p$ - $\alpha$  and  $p$ - $n$  interactions with an  $\alpha$ - $n$ - $n$  cluster distribution should be a good approximation to the  $p$ - ${}^6\text{He}$  interaction potential. The CF optical potential can be written as  $U_{CF} = \sum_{i=1,2} \int V_{pn_i} \rho_n(r_i) dr_i + \int V_{p\alpha} \rho_\alpha(r_\alpha) dr_\alpha$ , where  $V_{pX}$  includes both central and spin-orbit parts. In the actual calculation, a phenomenological optical potential that reproduces the  $p$ - ${}^4\text{He}$  elastic-scattering data at 72 MeV/nucleon [22] is used as the  $p$ - $\alpha$  interaction. Complicated effects in the  $p$ - $\alpha$  interaction, such as nonlocality originating from the exchange process, are considered to be simulated by the phenomenological optical potential, at least in part. The complex effective interaction CEG [23] is adopted as the  $p$ - $n$  interaction. Those interactions are folded with the  $\alpha$ - $n$ - $n$  distributions determined by using the Gaussian expansion method [24]. Details of the calculation will be reported elsewhere [25].

In Fig. 3, results of the CF calculation (solid lines) are compared with the  ${}^6\text{He}$  (circles) and  ${}^4\text{He}$  (squares) [22] data. The  ${}^4\text{He}$  data are plotted at the angle where momentum

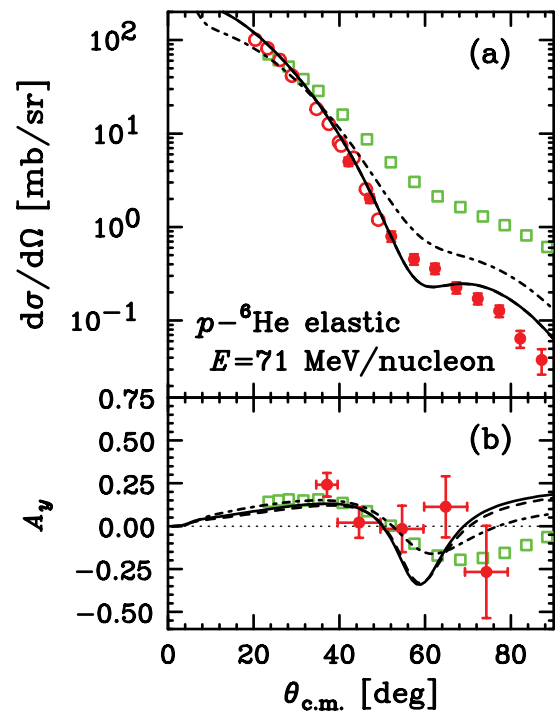


FIG. 3. (Color online) Present data compared with the cluster-folding calculations. Solid, dashed, and dot-dashed lines represent calculations with full,  $V_{pn;ls} = 0$ , and  $V_{pn;ls} = V_{pn;central} = 0$  interactions, respectively. Data for the  $p$ - ${}^4\text{He}$  scattering [22] (squares) are also shown.

transfer for  $p$ - ${}^6\text{He}$  is the same as that for the corresponding  $p$ - ${}^4\text{He}$  data. Although the angular distribution of  $d\sigma/d\Omega$  for  ${}^6\text{He}$  differs considerably from the more gradual one for  ${}^4\text{He}$ , the  $A_y$  data are similar to each other. The CF calculation reproduces both  $d\sigma/d\Omega$  and  $A_y$  reasonably, in particular, at  $\theta_{c.m.} \sim 35^\circ$ – $60^\circ$ .

To separate the valence neutron and the  $\alpha$ -core contributions, calculations with  $V_{pn;\ell s} = 0$  (dashed lines) and with  $V_{pn;\ell s} = V_{pn;\text{central}} = 0$  (dot-dashed lines) have been made. The latter corresponds to extraction of a pure  $\alpha$ -core contribution. As shown in Fig. 3, the  $p$ - $n$  central interaction causes a sizable effect on  $d\sigma/d\Omega$ . Because of the  $\alpha$ -core motion in  ${}^6\text{He}$ , matter distribution of the core part is wider than that of a bare  ${}^4\text{He}$  nucleus, while it is naturally narrower than that of  ${}^6\text{He}$  as a whole. Reflecting on this,  $d\sigma/d\Omega$  for the  $\alpha$ -core contribution appears between  ${}^4\text{He}$  and  ${}^6\text{He}$  data. It is also found that the spin-orbit interaction  $V_{pn;\ell s}$  gives negligible effects on  $d\sigma/d\Omega$  and  $A_y$ , which is consistent with predictions in Ref. [14]. Thus, from comparisons with CF, it is concluded that nuclear structure sensitivity of  $A_y$  does not originate from the direct valence neutron contribution, but from the  $\alpha$ -core contribution. The latter, which is affected by recoil of the valence neutrons, seems to be a possible key for understanding the behavior of  $A_y$ .

To summarize, we have performed an experiment to measure  $A_y$  and  $d\sigma/d\Omega$  in scattering of a neutron-rich  ${}^6\text{He}$  nucleus from protons, by using the newly developed polarized

proton solid target. The  $A_y$  data are obtained with a proton polarization determined by asymmetry in the  $p$ - ${}^4\text{He}$  scattering. We conclude, from comparisons with the microscopic folding model calculations, that (1) overall agreement between the present data and the 6BF calculation is found for the WS wave function. In particular, the  $d\sigma/d\Omega$  data at backward angles favor the existence of the halo structure in  ${}^6\text{He}$ ; (2) the data are reproduced by CF calculations reasonably well. The CF calculations show that direct contribution from the valence neutrons to analyzing power is negligibly small. Thus, nuclear structure effects on  $A_y$  may originate from the spatial distribution of the  $\alpha$  core in  ${}^6\text{He}$ , which is closely connected to the valence neutron distribution. This can be a possible key for understanding spin-orbit coupling in a neutron-rich  ${}^6\text{He}$  nucleus.

The present paper has demonstrated that the technique for polarizing protons in a low magnetic field can open new possibilities for exploring the physics of unstable nuclei. Experiments with the target would provide fruitful results in future radioactive nuclear beam facilities.

We thank the RIKEN and CNS staffs for the operation of the accelerators during the measurement. One of the authors (S.S.) expresses his gratitude for financial support by a Grant-in-Aid for JSPS Fellows (No. 18-11398). This work was supported by the Grant-in-Aid No. 17684005 of the Ministry of Education, Culture, Sports, Science, and Technology of Japan.

- 
- [1] C. Oxley *et al.*, *Phys. Rev.* **91**, 419 (1953).  
 [2] O. Chamberlain *et al.*, *Phys. Rev.* **102**, 1659 (1956).  
 [3] E. Fermi, *Il Nuovo Cimento* **10**, 407 (1954).  
 [4] A. Korshennikov *et al.*, *Nucl. Phys. A* **617**, 45 (1997).  
 [5] R. Wolski *et al.*, *Phys. Lett. B* **467**, 8 (1999).  
 [6] M. D. Cortina-Gil *et al.*, *Phys. Lett. B* **401**, 9 (1997).  
 [7] A. Lagoyannis *et al.*, *Phys. Lett. B* **518**, 27 (2001).  
 [8] P. Egelhof *et al.*, *Eur. Phys. J. A* **15**, 27 (2002).  
 [9] G. D. Alkhazov *et al.*, *Nucl. Phys. A* **712**, 269 (2002).  
 [10] S. Goertz, W. Meyer, and G. Reicherz, *Prog. Part. Nucl. Phys.* **49**, 403 (2002), and references therein.  
 [11] T. Wakui, in *Proceedings of the XIth International Workshop on Polarized Ion Source and Polarized Gas Targets 2005*, edited by T. Uesaka, H. Sakai, A. Yoshimi, and K. Asahi (World Scientific, Singapore, 2007), p. 49; T. Uesaka *et al.*, *Nucl. Instrum. Methods A* **526**, 186 (2004).  
 [12] A. Henstra, P. Dirksen, and W. T. Wenckebach, *Phys. Lett. A* **134**, 134 (1988).  
 [13] M. Hatano *et al.*, *Eur. Phys. J. A* **25**, 255 (2005).  
 [14] R. Crespo and A. M. Moro, *Phys. Rev. C* **76**, 054607 (2007).  
 [15] T. Kubo *et al.*, *Nucl. Instrum. Methods B* **70**, 309 (1992).  
 [16] T. Wakui *et al.*, *Nucl. Instrum. Methods A* **550**, 521 (2005).  
 [17] H. Togawa and H. Sakaguchi, RCNP Annual Report 1 (1987).  
 [18] R. Henneck *et al.*, *Nucl. Phys. A* **571**, 541 (1994).  
 [19] S. V. Stepanov *et al.*, *Phys. Lett. B* **542**, 35 (2002).  
 [20] S. P. Weppner, O. Garcia, and Ch. Elster, *Phys. Rev. C* **61**, 044601 (2000).  
 [21] K. Amos *et al.*, *Adv. Nucl. Phys.* **25**, 275 (2000).  
 [22] S. Burzynski *et al.*, *Phys. Rev. C* **39**, 56 (1989).  
 [23] N. Yamaguchi, S. Nagata, and T. Matsuda, *Prog. Theor. Phys.* **70**, 459 (1983).  
 [24] E. Hiyama, Y. Kino, and M. Kamimura, *Prog. Part. Nucl. Phys.* **51**, 223 (2003).  
 [25] S. Sakaguchi, Y. Iseri *et al.* (in preparation).